

Two-Dimensional Triple-Resonance HCNCH Experiment for Direct Correlation of Ribose H1' and Base H8, H6 Protons in ¹³C, ¹⁵N-Labeled RNA Oligonucleotides

Vladimír Sklenář,^{*†} Robert D. Peterson, Marita R. Rejante, Edmond Wang, and Juli Feigon^{*}

Department of Chemistry and Biochemistry and Molecular Biology Institute, University of California Los Angeles, California 90024

Received August 25, 1993

With the recent advent of methods for obtaining ¹³C and ¹⁵N uniformly labeled ribonucleotides,^{1,2} it is now possible to apply double- and triple-resonance NMR methods to obtain assignments and ultimately determine the structures of relatively large RNA molecules. Several double-resonance ¹H–¹³C and ¹H–¹⁵N experiments in labeled RNA have now been reported, for the assignment of ribose spin systems or identification of base proton resonances.^{2–6} We have recently shown that the H1' ribose protons can be correlated with aromatic H8 and H6 protons in the same nucleotide by determining the connectivities H1'–C1'–N9/N1 and H8/H6–C8/C6–N9/N1 in two separate 2D or 3D triple-resonance experiments.⁷ In this communication we present an alternative approach which allows unambiguous assignment of intranucleotide H1'–H8 and H1'–H6 connectivities by a single 2D triple-resonance HCNCH experiment. Since the aromatic and H1' regions of the proton spectrum are relatively well resolved even for RNA molecules as large as the 30-base ribonucleotide used in these studies, the two-dimensional experiment is usually adequate for identifying the intranucleotide H1'–H8/H6 correlations. Once the intranucleotide correlations are made, they can be combined with internucleotide H1'–H8/H6 connectivities observed in NOESY⁸ spectra to obtain sequence specific assignments⁹ along the RNA strand.

The pulse scheme (Figure 1) utilizes four consecutive INEPT¹⁰ steps to transfer the H1' proton coherence along the pathways H1'–C1'–N9–C8–H8 in purine and H1'–C1'–N1–C6–H6 in pyrimidine nucleotides (Figure 2). Because of complex heteronuclear *J*-coupling networks in purine and pyrimidine bases, the INEPT steps have to be designed as semiselective to direct the transfers along the desired coherence pathways. The basic principles are now briefly discussed using the product operator formalism.^{11–13} A standard {¹H–¹³C} INEPT correlation sequence^{14,15} is used to label the H1' magnetization by its proton

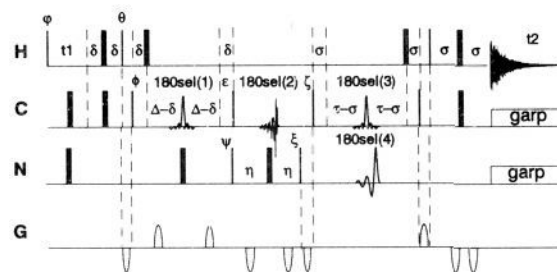


Figure 1. The pulse scheme of the 2D HCNCH experiment. The narrow and broad filled bars represent the nonselective 90° and 180° pulses, respectively. The delay intervals are set to $\delta = 1.6$ ms, $\sigma = 1.25$ ms, $\Delta = 19.6$ ms, $\eta = 18$ ms, $\tau = 19$ ms (for explanation, see text). The 180° semiselective pulses (180°sel(*n*)) as used at 500 MHz are (1) ¹³C 4-ms REBURP refocusing pulse¹⁶ covering the range of C1' (~88–96 ppm), (2) ¹³C 4-ms IBURP2 inversion pulse¹⁶ with additional cosine modulation^{17,18} for simultaneous inversion of C1' (88–96 ppm) and C6/C8 (136.5–144.5 ppm), (3) ¹³C 4-ms REBURP refocusing pulse¹⁶ covering the range of C6 and C8 (~136.5–144.5 ppm), and (4) ¹⁵N 2-ms IBURP2 pulse¹⁶ centered at 160 ppm covering the range of N1 and N9 (142–176 ppm). Phase cycling: $\phi = x$; $\theta = x, x, -x, -x$; $\psi = 4x, 4(-x)$; $\xi = 8x, 8(-x)$; $\zeta = 16x, 16(-x)$; $\theta = y, -y$; $\epsilon = 16(x), 16(-x)$. All other pulses are applied along the *x*-axis. In addition, ϕ is phase-cycled to obtain States-TPP1²⁸ *t*₁-quadrature detection. The 1-ms gradient pulses (800- μ s gradient pulse shaped to a 1% truncated sine envelope and 200 μ s for field recovery) are employed with amplitudes $-6/3/3/-6/3/3/12/-3/3$ G/cm. The asynchronous ¹³C and ¹⁵N GARP decoupling²⁹ is used to suppress the heteronuclear spin–spin interactions during the *t*₂-acquisition.

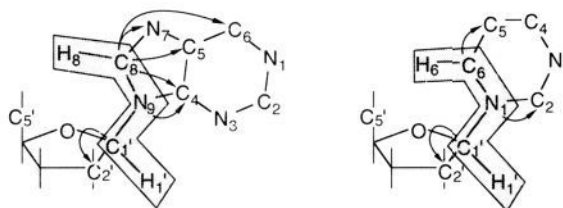


Figure 2. Schematic illustrating the coherence transfer pathways of the HCNCH experiment for purine (left) and pyrimidine (right) ribonucleotides (shaded region). Some of the alternative coherence transfer pathways involving C and N which are suppressed by selective excitation during the experiment are indicated by the arrows.

chemical shift and to transfer the coherence to the C1'. The following delay $2\delta = 1/2J_{H1',C1'}$ is applied to refocus the C1' coherence, which is antiphase with respect to the H1' from which it originates: $(2H1'_z C1'_y \cos(\omega_{H1'} t_1) \rightarrow C1'_x \cos(\omega_{H1'} t_1))$. During the interval $2\Delta \sim 1/2J_{C1',N9} \sim 1/2J_{C1',N1}$, the in-phase C1'_{*x*} magnetizations evolve into the antiphase coherences $2N9_z C1'_y \cos(\omega_{H1'} t_1)$ and $2N1_z C1'_y \cos(\omega_{H1'} t_1)$ due to the C1'–N9 and C1'–N1 scalar interactions. The C1'–C2' scalar interaction is decoupled by applying a semiselective ¹³C 180° refocusing pulse to the region of C1' carbons. The {¹³C–¹⁵N} INEPT step transfers the C1' magnetizations to the glycosidic nitrogens N9 and N1. The following interval 2η is used to refocus the N9 and N1 magnetizations, which are now antiphase with respect to their originating C1'. At the same time, the nitrogen coherences evolve due to the N9–C8 and N1–C6 scalar interactions and become antiphase with respect to the next coupling partners C8 or C6 along the desired transfer pathways. The relevant terms are $2N9_y C8_z \cos(\omega_{H1'} t_1)$ and $2N1_y C6_z \cos(\omega_{H1'} t_1)$. The delay 2η is set to the best compromise for the different coupling constants $J_{C1',N9}$ and $J_{C1',N1}$ (~11–12 Hz), $J_{N9,C8}$ (~4–8 Hz), and $J_{N1,C6}$ (~13 Hz). A pair of 180° pulses is applied in the middle of this interval. The ¹⁵N 180° pulse refocuses the ¹⁵N chemical shift evolution and decouples the two-bond scalar interactions with *J*-coupled protons H1', H8, and H6. The ¹³C 180° pulse is made double semiselective to prevent the *J*-evolution due to the irrelevant scalar interactions N1–C2 and N1–C5 in pyrimidines and N9–

* Corresponding authors.

† Also from the Institute of Scientific Instruments, Academy of Sciences of the Czech Republic, 612 64 Brno, Czech Republic.

(1) Nikonowicz, E. P.; Sirt, A.; Legault, P.; Jucker, F. M.; Baer, L. M.; Pardi, A. *Nucleic Acids Res.* **1992**, *20*, 4507–4513.

(2) Batey, R. T.; Inada, M.; Kujawinski, E.; Puglisi, J. D.; Williamson, J. R. *Nucleic Acids Res.* **1992**, *20*, 4515–4523.

(3) Nikonowicz, E. P.; Pardi, A. *Nature* **1992**, *355*, 184–186.

(4) Nikonowicz, E. P.; Pardi, A. *J. Am. Chem. Soc.* **1992**, *114*, 1082–1083.

(5) Michnicka, M. J.; Harper, J. W.; King, G. C. *Biochemistry* **1993**, *32*, 395–400.

(6) Nikonowicz, E. P.; Pardi, A. *J. Mol. Biol.* **1993**, *232*, 1141–1156.

(7) Sklenář, V.; Peterson, R. D.; Rejante, M. R.; Feigon, J. *J. Biomol. NMR*, in press.

(8) Kumar, A.; Ernst, R. R.; Wüthrich, K. *Biochem. Biophys. Res. Commun.* **1980**, *95*, 1–6.

(9) Wüthrich, K. *NMR of Proteins and Nucleic Acids*; John Wiley & Sons: New York, NY, 1986.

(10) Morris, G. A.; Freeman, R. *J. Am. Chem. Soc.* **1979**, *101*, 760–762.

(11) Sorensen, O. W.; Eich, G. W.; Levitt, M. H.; Bodenhausen, G.; Ernst, R. R. *Prog. Nucl. Magn. Reson. Spectrosc.* **1983**, *16*, 163–192.

(12) van de Ven, F. J. M.; Hilbers, C. W. *J. Magn. Reson.* **1983**, *54*, 512–520.

(13) Packer, K. J.; Wright, K. M. *Mol. Phys.* **1983**, *50*, 797–813.

(14) Maudsley, A. A.; Muller, L.; Ernst, R. R. *J. Magn. Reson.* **1977**, *28*, 463–469.

(15) Bodenhausen, G.; Freeman, R. *J. Magn. Reson.* **1977**, *28*, 471–476.

C4 in purines. In our implementation, the IBURP2 shaped pulse¹⁶ is modulated by the cosine function^{17,18} to invert the ¹³C z -magnetization in the chemical shift range of the C1' and C8/C6 carbons simultaneously. After transferring the antiphase nitrogen magnetizations to carbons C8 and C6, the interval $2\tau \sim 1/2J_{C8,N9} \sim 1/2J_{C6,N1}$ is used to refocus the ¹³C magnetizations. At the beginning of this interval, the ¹³C magnetizations are antiphase with respect to their originating nitrogens N9 and N1. During this delay the competitive ¹³C–¹³C and ¹³C–¹⁵N scalar interactions C8–C4, C8–C5, C8–C6, C6–C5, C6–C2, and C8–N7 are decoupled by the semiselective ¹³C and ¹⁵N 180° pulses. These pulses are applied to refocus only pyrimidine C6 and purine C8 carbons and to invert the z -magnetization of the N1 and N9, while leaving the C4, C5, C6, and N7 resonances in purines and the C5 and C2 resonances in pyrimidines unaffected. In addition, during the delay $2\sigma \sim 1/2J_{C8,H8} \sim 1/2J_{C6,H6}$, the ¹³C magnetizations are allowed to evolve due to the scalar interactions with their directly bonded protons H8 and H6. The final $\{^{13}\text{C}-^1\text{H}\}$ INEPT step transfers the ¹³C magnetizations to protons H8 and H6, which are detected after the 2σ refocusing interval with simultaneous ¹³C and ¹⁵N broadband decoupling. The relevant product operator terms at the beginning of the t_2 detection period are $\text{H8}_x \cos(\omega_{\text{H1}' t_1})$ and $\text{H6}_x \cos(\omega_{\text{H1}' t_1})$. To minimize the required phase cycling, gradient pulses are applied to purge unwanted coherences during the short delays (~ 1 ms) when the magnetizations of interest are converted into the zz -orders.^{19–21} In order to remove imperfections of the refocusing 180° pulses, two symmetrical gradients are used on both sides to generate a perfect echo.^{20,21} The pulse sequence yields pure-phase 2D NMR spectra which correlate H1' resonances in the F1 to H8 and H6 resonances in the F2 dimension.

An HCNCH spectrum of a 1.2 mM sample of RBE3, a 30-nucleotide RNA derived from the RRE (rev response element) which contains the high-affinity binding site for the Rev protein of the HIV-1,^{22,23} is shown in Figure 3a. The RNA folds into a stem–internal loop–stem–hairpin loop structure (Scheme I). The relatively large size of this RNA provides a good test of the applicability of the method. The sensitivity of the HCNCH experiment is limited by the small coupling constants involved ($J_{C,N} \sim 4\text{--}13$ Hz) and the short T_2 in ¹³C-labeled RNA oligonucleotides. Nevertheless, all of the intranucleotide H1'–H8, H6 correlations are observed in this spectrum with the exception of three purine residues in the internal loop, which also give rise to only weak or no NOEs in the NOESY spectrum due to

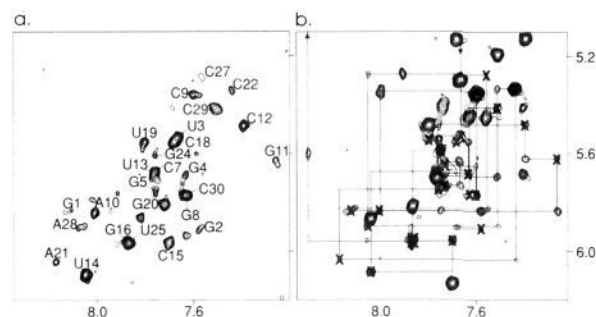
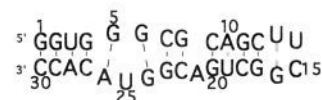


Figure 3. Portion of 500-MHz (Bruker AMX 500) two-dimensional (a) HCNCH and (b) NOESY spectra of ¹³C,¹⁵N-labeled RBE3 at 40 °C showing the cross peaks between the base proton and H1' resonances. The intranucleotide H8, H6–H1' connectivities observed in the HCNCH spectrum are marked by X in the NOESY spectrum. There are some additional cross peaks in the HCNCH spectrum which are not observed in the NOESY spectrum; these are probably due to a lower molecular weight impurity. The HCNCH spectrum was acquired with 512 and 360 complex points in t_2 and t_1 , respectively, 96 scans per t_1 increment, and a spectral width of 2500 Hz in both dimensions, was apodized with a 60° and 75° shifted squared sine bell in t_2 and t_1 , and was zero-filled to 1K in both dimensions. The NOESY spectrum was acquired on the same sample with $\tau_m = 300$ ms using the standard pulse sequence⁸ and States-TPPI phase cycling and ¹⁵N and ¹³C decoupling during t_1 and t_2 .

Scheme I



conformational averaging, and G17, due to an upfield shift of the H1' outside the selected region. The observed intensities of the purine cross peaks are consistently lower than those from the pyrimidines because the purine C8–N9 coupling constants are substantially smaller than the pyrimidine C6–N1 coupling constants. The intranucleotide connectivities obtained from the HCNCH spectrum are labeled on the NOESY spectrum of RBE3 in Figure 3b.²⁴ The unambiguous identification of the intranucleotide connectivities greatly simplifies the sequential assignment procedure, since intranucleotide NOEs can now be unambiguously distinguished from internucleotide NOEs. The HCNCH spectrum was obtained in 15.5 h on a 1.2 mM RNA sample and thus provides a rapid and sensitive method for obtaining intranucleotide scalar connectivities between ribose and base in ¹³C,¹⁵N-double-labeled RNA oligonucleotides.

Acknowledgment. This work was supported by NIH Grants P01 GM 39558-07 and R01 GM48123-02 to J.F.; NIH Pre-doctoral Training Grant GM07185 to R.D.P.; and instrumentation funds from NSF Grant BIR 9115862 to J.F.

(24) The cross peaks in the sequential assignments which are missing in the NOESY spectrum of the ¹³C,¹⁵N-labeled RBE3 are observed in the NOESY spectra of a higher concentration sample of unlabeled RBE3.

(25) Milligan, J. F.; Groebe, D. R.; Witherell, G. W.; Uhlenbeck, O. C. *Nucleic Acids Res.* **1987**, *15*, 8783–8798.

(26) Heus, H. A.; Pardi, A. *J. Mol. Biol.* **1991**, *217*, 113–124.

(27) Wyatt, J. R.; Chastain, M.; Puglisi, J. D. *BioTechniques* **1991**, *11*, 764–769.

(28) Marion, D.; Ikura, M.; Tschudin, R.; Bax, A. *J. Magn. Reson.* **1989**, *85*, 393–399.

(29) Shaka, A. J.; Barker, P.; Freeman, R. *J. Magn. Reson.* **1985**, *64*, 547–552.

(16) Geen, H.; Freeman, R. *J. Magn. Reson.* **1991**, *93*, 93–141.

(17) Tomlinson, B. L.; Hill, H. D. W. *J. Chem. Phys.* **1973**, *59*, 1775–1784.

(18) Konrat, R.; Burghardt, I.; Bodenhausen, G. *J. Am. Chem. Soc.* **1991**, *113*, 9135–9140.

(19) Brühwiler, D.; Wagner, G. *J. Magn. Reson.* **1986**, *69*, 546–551.

(20) Bax, A.; Pochapsky, S. *J. Magn. Reson.* **1992**, *99*, 638–643.

(21) Sklenář, V.; Piotto, M.; Leppik, R.; Saudek, V. *J. Magn. Reson. Ser. A* **1993**, *102*, 241–245.

(22) Bartel, D. P.; Zapp, M. L.; Green, M. R.; Szostak, J. W. *Cell* **1991**, *67*, 529–536.

(23) RBE3 was enzymatically synthesized on a DNA template using T7 RNA polymerase to incorporate labeled NTPs following procedures described by Milligan *et al.*²⁵ and scaled up to yield NMR quantities.^{26,27} The ¹³C,¹⁵N-labeled NTPs were prepared from RNA isolated from *Escherichia coli* grown in ¹³C-glucose and ¹⁵N-(NH₄)₂SO₄ containing media¹ following the procedures of Batey *et al.*² The RNA was purified by polyacrylamide gel electrophoresis and electroelution, followed by ethanol precipitation and dialysis (Centricon-SR 3 filters) in 10 mM phosphate, pH 6.0, 100 mM NaCl. The NMR sample was 1.2 mM RBE3 in 450 μ L.